Electron parallel closures for arbitrary collisionality

Journal-ref: Phys. Plasmas 21, 112116 (2014); 22, 129901 (2015)

Jeong-Young Ji* and Eric D. Held

Department of Physics, Utah State University, Logan, Utah 84322

Abstract

Electron parallel closures for heat flow, viscosity, and friction force are expressed as kernel-weighted integrals of thermodynamic drives, the temperature gradient, relative electron-ion flow velocity, and flow-velocity gradient. Simple, fitted kernel functions are obtained for arbitrary collisionality from the 6400 moment solution and the asymptotic behavior in the collisionless limit. The fitted kernels circumvent having to solve higher order moment equations in order to close the electron fluid equations. For this reason, the electron parallel closures provide a useful and general tool for theoretical and computational models of astrophysical and laboratory plasmas.

*Electronic address: j.ji@usu.edu

I. INTRODUCTION

Plasma fluid closures are essential to developing sets of fluid equations that capture kinetic effects in astrophysical and laboratory plasmas. A complete set of closures for the Maxwellian moment equations (for density n, temperature T, and flow velocity $\mathbf{V}$) exists only for high collisionality [1]. At low collisionality, particle free streaming parallel to the magnetic field becomes significant and closures are affected by thermodynamic drives along the field line. Consequently, the closures take on an integral form, as they do in the collisionless limit [2, 3].

Obtaining quantitative parallel closures for arbitrary collisionality requires accurate collision operators. As a crude approximation, a Krook type operator was adopted in the 3+1 closure model of Ref. [4]. As better approximations, Lorentz type operators were used to obtain closures in wave number space [5] and approximate integral closures for the heat flow due to a temperature gradient [6] and viscosity due to a flow velocity gradient [7].

Recently, the exact linearized Coulomb collision operators were analytically calculated for an infinite hierarchy of moment equations [8, 9]. These moment equations were truncated, linearized, and solved to produce integral parallel closures for arbitrary collisionality [10, 11]. The resultant integral heat flow closure was tested in numerical calculations of energy confinement in the Sustained Spheromak Physics Experiment and yielded modestly better agreement with experimental measurements than Braginskii's diffusive heat flow [10]. This integral heat flow was also used to capture kinetic effects in the JET scrape-off layer [12].

Practical use of the integral closures is complicated by the need to express the kernel functions for arbitrary collisionality. Kernels obtained from N-moment equations are sums of $N/2$ exponential functions. At low collisionality, large N is needed for convergent results. In the collisionless limit, however, simple analytical expressions for the kernels exist [2, 3, 5, 13]. In this paper, we provide simple kernel functions that map onto the $N = 6400$ kernels in the convergent regime and the collisionless kernels in the nonconvergent regime.

II. PARALLEL MOMENT EQUATIONS AND CLOSURES

For a strong magnetic field, parallel moment equations can be obtained by taking moments of the drift kinetic equation [14] or, equivalently, by taking the parallel component of general moment equations [15]. For no magnetic field, an inhomogeneous system along one direction

produces similar moment equations. The linearized parallel moment equations are [10, 11]

$$\sum_{B=1}^{N} \Psi_{AB} \frac{\partial n_B}{\partial \eta} = \sum_{B=1}^{N} C_{AB} n_B + g_A, \tag{1}$$

where the moment index $A = 1, 2, \cdots, N$ enumerates $(l,k) = (0,2), \cdots, (0, K+1), (1,1), \cdots, (1,K), (2,0), \cdots, (L-1, K-1)$. The indices l and k denote the Legendre polynomial and Laguerre-Sonine polynomial orders with $N = LK$. The arclength ℓ along a magnetic field line is normalized by the mean free path, $d\eta = d\ell/\lambda_{\rm mfp}$ or $\eta(\ell) = \int^{\ell} d\ell'/\lambda_{\rm mfp}(\ell')$, where $\lambda_{\rm mfp} = v_T \tau$, the electron thermal speed $v_T = \sqrt{2T/m}$, and the electron-electron collision time $\tau = \tau_{\rm ee} = 6\sqrt{2}\pi^{3/2}\epsilon_0^2\sqrt{m}T^{3/2}/ne^4 \ln\Lambda$. Here m is the electron mass, e is the electron charge, and $\ln\Lambda$ is the Coulomb logarithm. The collision matrix C_{AB} includes the electron-electron and electron-ion collision terms. For electrons, the nonvanishing thermodynamic drives g_A include the parallel temperature gradient $\partial_\parallel T$, the relative parallel flow velocity $V_{{\rm ei}\parallel}$, and the parallel component of the rate of strain tensor $W_\parallel = \mathbf{bb} : \mathsf{W}$, $(\mathsf{W})_{\alpha\beta} = \partial_\alpha V_\beta + \partial_\beta V_\alpha - \frac{2}{3}\delta_{\alpha\beta}\nabla\cdot\mathbf{V}$. The non-Maxwellian moments n_A include the parallel heat flux density $h_\parallel$, parallel viscosity $\pi_\parallel$, and parallel friction force density $R_\parallel$.

The linear system (1) with constant matrices Ψ and C is solved by computing the eigensystem of $\Psi^{-1}C$ [10, 11]. The desired particular solution is

$$h_\parallel(\ell) = T v_T \int d\eta' \Big(-\frac{1}{2} K_{hh} \frac{n}{T}\frac{dT}{d\eta'} + K_{hR} Z n \frac{V_{{\rm ei}\parallel}}{v_T} - K_{h\pi}\frac{3}{4} n\tau W_\parallel \Big), \tag{2}$$

$$R_\parallel(\ell) = -\frac{mn}{\tau_{\rm ei}} V_{{\rm ei}\parallel} + \frac{m v_T}{\tau_{\rm ei}} \int d\eta' \Big(-K_{Rh}\frac{n}{2T}\frac{dT}{d\eta'} + K_{RR} Z n \frac{V_{{\rm ei}\parallel}}{v_T} - K_{R\pi}\frac{3}{4} n\tau W_\parallel \Big), \tag{3}$$

$$\pi_\parallel(\ell) = T \int d\eta' \Big(-K_{\pi h}\frac{n}{T}\frac{dT}{d\eta'} + 2K_{\pi R} Z n \frac{V_{{\rm ei}\parallel}}{v_T} - K_{\pi\pi}\frac{3}{4} n\tau W_\parallel \Big), \tag{4}$$

where $\int d\eta' K_{AB} g_B$ means $\int d\eta' K_{AB}(\eta - \eta') g_B(\ell')$ with $\eta = \eta(\ell)$ and $\eta' = \eta(\ell')$. The N-moment kernels are given by

$$K_{AD}(\eta) = \begin{cases} -\displaystyle\sum_{\{B|k_B>0\}}^{N} \gamma_{AD}^B e^{+k_B\eta}, & \eta < 0, \\ +\displaystyle\sum_{\{B|k_B<0\}}^{N} \gamma_{AD}^B e^{+k_B\eta}, & \eta > 0, \end{cases} \tag{5}$$

where eigenvalues k_B of $\Psi^{-1}C$ appear in positive and negative pairs. The coefficients γ_{AD}^B are determined by the eigenvector components and satisfy $\gamma_{AD}^B = \gamma_{DA}^B$ and

$$\gamma_{AD}^{-B} = \begin{cases} -\gamma_{AD}^B, & AD = hh, hR, RR, \pi\pi \equiv \text{even}, \\ +\gamma_{AD}^B, & AD = h\pi, R\pi \equiv \text{odd}, \end{cases} \tag{6}$$

where $-B$ denotes the moment index corresponding to $-k_B$. Therefore $K_{AD} = K_{DA}$ and the kernels are even or odd functions of η.

Since the kernels are computed from a truncated system of N moment equations, convergence should be checked as N increases. We start with $N = 100$ ($L = 10$ and $K = 10$) and go to $N = 6400$ ($L = 80$ and $K = 80$) by quadrupling N (doubling both L and K). The convergence of the kernel functions is shown in Fig. 1. In the collisional limit, the drives are effectively constant and the areas $\int K_{AB}(\eta)d\eta$ become the classical closure coefficients. The areas change little with increasing N, indicating that the $N = 100$ ($K = 10$) moment calculation accurately yields the classical coefficients. In general, the kernels converge for $\eta \gtrsim \eta_c$, where η_c decreases with increasing N.

To study the convergence of closures as collisionality varies, we consider sinusoidal drives, $T = T_0+T_1 \sin\varphi$, $V_\parallel = V_0+V_1 \sin\varphi$, and $V_{ei\parallel} = V_{ei} \cos\varphi$, where $\varphi = 2\pi\ell/\lambda+\varphi_0 = k\eta+\varphi_0$. The wave number normalized by the mean free path, $k = 2\pi\lambda_{mfp}/\lambda$, measures the inverse collisionality. Note that although λ and φ_0 (and hence φ) may be different for each drive, we have used the same symbols for convenience. Assuming that n and $v_T \approx \sqrt{2T_0/m}$ are constant and that $\mathbf{V}_\perp = 0$, for simplicity, the closures can be obtained by evaluating the integrals,

$$\int K_{AD}(\eta-\eta')\cos\varphi' d\eta' = \begin{cases} \hat{K}_{AD}\cos\varphi, & AD = \text{even}, \\ \hat{K}_{AD}\sin\varphi, & AD = \text{odd}, \end{cases} \tag{7}$$

where $\varphi' = k\eta' + \varphi_0$ and

$$\hat{K}_{AD} = \begin{cases} \sum_{B=1}^{N} \dfrac{-\gamma_{AD}^B k_B}{k_B^2+k^2}, & AD = \text{even}, \\ \sum_{B=1}^{N} \dfrac{\gamma_{AD}^B k}{k_B^2+k^2}, & AD = \text{odd}. \end{cases} \tag{8}$$

Upon linearization the closures become

$$h_\parallel(\ell) = -\frac{1}{2}nT_1 v_T \hat{h}_h \cos\varphi + nT_0 Z V_{ei}\hat{h}_R \cos\varphi - nT_0 V_1 \hat{h}_\pi \sin\varphi, \tag{9}$$

$$R_\parallel(\ell) = -nT_1 \frac{2\pi}{\lambda}\hat{R}_h \cos\varphi - \frac{mnV_{ei}}{\tau_{ei}}\hat{R}_R \cos\varphi - nmV_1 \frac{2\pi v_T}{\lambda}\hat{R}_\pi \sin\varphi, \tag{10}$$

$$\pi_\parallel(\ell) = -nT_1\hat{\pi}_h \sin\varphi + 2nT_0 Z\frac{V_{ei}}{v_T}\hat{\pi}_R \sin\varphi - nT_0\frac{V_1}{v_T}\hat{\pi}_\pi \cos\varphi, \tag{11}$$

with the dimensionless closures defined by $\hat{h}_h = k\hat{K}_{hh}$, $\hat{h}_R = Z\hat{K}_{hR} = \hat{R}_h$, $\hat{h}_\pi = k\hat{K}_{h\pi} = \hat{\pi}_h$, $\hat{R}_R = 1 - \hat{K}_{RR}$, $\hat{R}_\pi = Z\hat{K}_{R\pi} = \hat{\pi}_R$, and $\hat{\pi}_\pi = k\hat{K}_{\pi\pi}$.

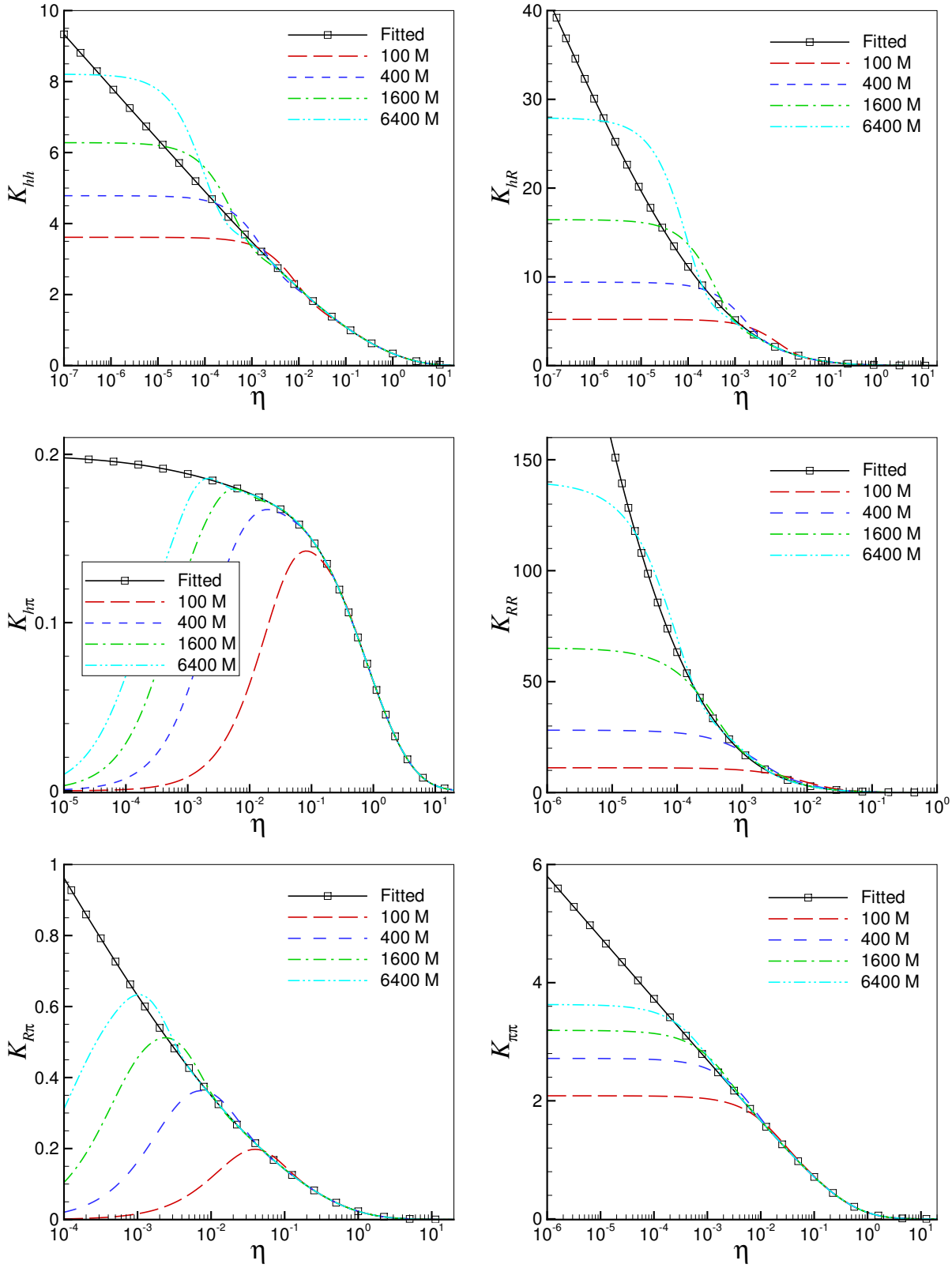

Figure 1: (Color online) Kernel functions for ion charge $Z = 1$ computed from N =100 (red, long-dashed), 400 (blue, short-dashed), 1600 (green, dash-dotted), and 6400 (cyan, dash-dot-dotted). The fitted kernels (black, solid with squares) are also shown.

Figure 2 shows the dimensionless closures as functions of k. For a given gradient scale length λ, as $\lambda_{\rm mfp}$ increases (collisionality decreases), k increases. For small k (high collisionality), the closures are convergent with a small number of moments (see Fig. 2). Errors in Braginskii's closures are largest for h_h, the heat flow due to the temperature gradient. This error is 16% for $k \sim 0.1$ ($\epsilon \equiv \lambda_{\rm mfp}/\lambda \sim 0.02$) and 100% for $k \sim 0.4$ ($\epsilon \sim 0.06$). These results agree well with the prediction of the higher-order Chapman-Enskog theory in Ref. [8]. In Figs. 1 and 2, the convergence of closures is attributed to the convergence of the kernels for $\eta \gtrsim \eta_{\rm c}$. Note that $\eta_{\rm c}$ decreases as N increases. As k increases, convergent closures are obtained by using more moments. Although, for a given k, there exists N that yields convergent results, it is more profitable to invoke the collisionless theory. Instead of increasing N (decreasing $\eta_{\rm c}$) to obtain accurate kernels for smaller η, we consider mapping onto the collisionless kernels for $\eta \ll 1$ in order to determine fitted kernels that are approximately valid for arbitrary collisionality.

III. SIMPLE FITTED KERNEL FUNCTIONS

The kernel functions obtained from 6400 moment equations include 3200 terms [see Eq. (5)]. Incorporating those eigenvalues and the corresponding coefficients in simulations is impractical. Furthermore, the kernels are still inaccurate for $k \gtrsim 80$ near the collisionless limit. Therefore, it is convenient to find simple fitted functions that (i) accurately represent the moment solutions in the convergent regime ($k \lesssim 80$), and (ii) have the correct asymptotic behavior in the collisionless limit. This approach yields kernels that are nearly exact for arbitrary collisionality.

In the collisional limit ($\lambda_{\rm mfp} \to 0$), the parallel closures are described by Braginskii's theory ($K = 2$ calculation [1], here convergent values [16] are shown) with ion charge $Z = 1$,

$$h_\parallel = -3.203\frac{nT\tau_{\rm ee}}{m}\partial_\parallel T + 0.703nTV_{{\rm ei}\parallel}, \tag{12}$$

$$R_\parallel = -0.703n\partial_\parallel T - 0.506\frac{mn}{\tau_{\rm ei}}V_{{\rm ei}\parallel}, \tag{13}$$

$$\pi_\parallel = -0.978nT\tau_{\rm ee}\frac{3}{4}W_\parallel. \tag{14}$$

Noting that $\int d\eta' K_{AD}(\eta-\eta')g_D(\ell') \to \hat{\kappa}_{AD}g_D(\ell)$ in the collisional limit, the fitted kernels should

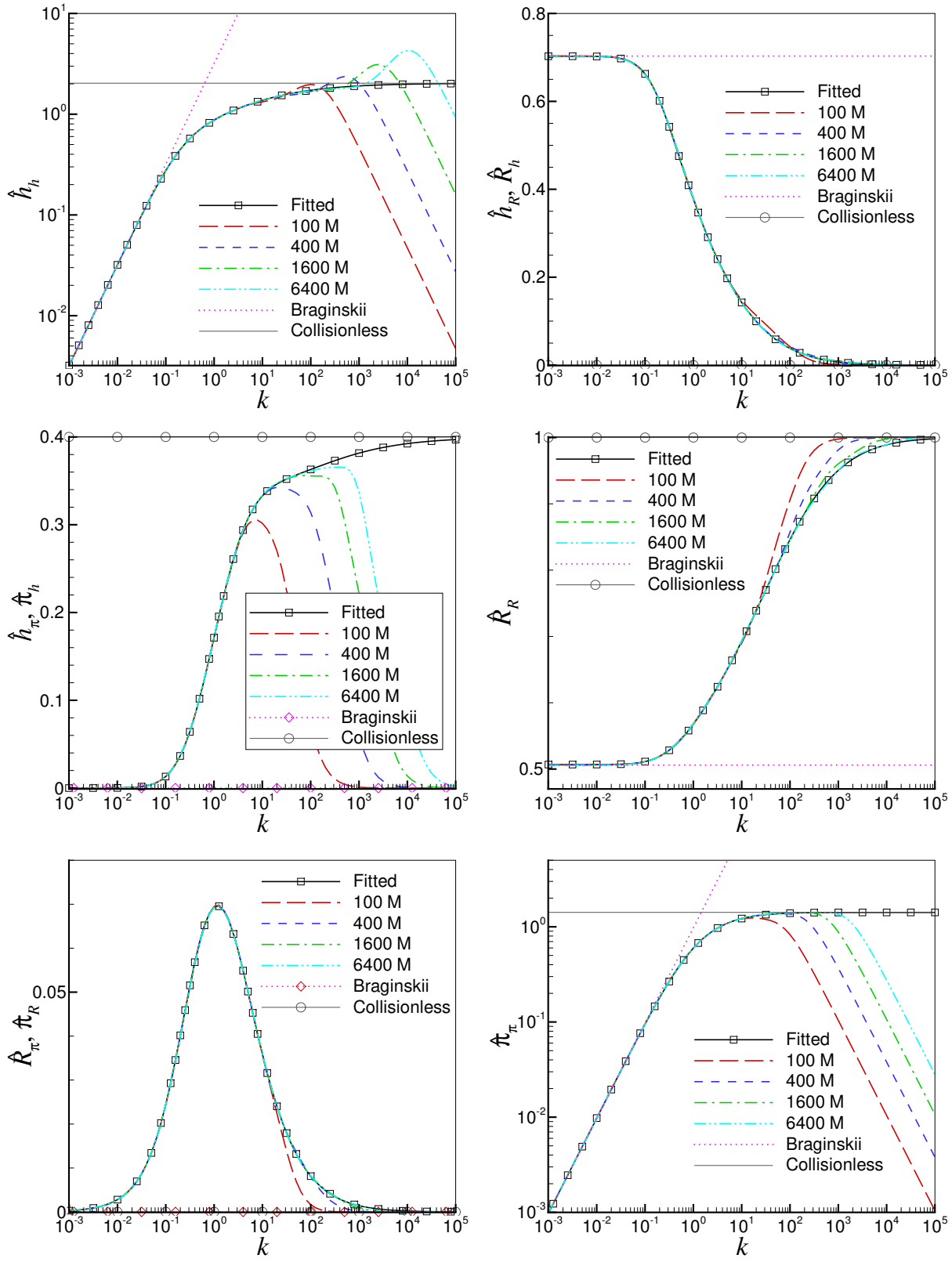

Figure 2: (Color online) Closures for sinusoidal drives computed for various N and fitted kernels in Fig. 1. The Braginskii (red, dotted [with diamonds]) and collisionless (gray, thin solid [with squares]) closures are also shown.

satisfy

$$\int_{-\infty}^{\infty} d\eta \begin{pmatrix} K_{hh}(\eta) \\ K_{hR}(\eta) \\ K_{RR}(\eta) \\ K_{\pi\pi}(\eta) \end{pmatrix} = \begin{pmatrix} 3.203 \\ 0.703 \\ 0.494 \\ 0.978 \end{pmatrix}. \tag{15}$$

The coefficients connecting $h_\parallel$ ($\pi_\parallel$) to $W_\parallel$ ($\partial_\parallel T$) and $R_\parallel$ ($\pi_\parallel$) to $W_\parallel$ ($V_{\mathrm{ei}\parallel}$) in Eqs. (12)-(14) vanish because the corresponding kernels are odd functions. However, we evaluate the integrals over $[0, \infty)$ to make the fitted kernels satisfy

$$\int_{0}^{\infty} d\eta \begin{pmatrix} K_{h\pi}(\eta) \\ K_{R\pi}(\eta) \end{pmatrix} = \begin{pmatrix} 0.264 \\ 0.104 \end{pmatrix}. \tag{16}$$

Finally, the asymptotic behavior of the kernels for small η can be obtained from closures in the collisionless limit [13]. For $\eta \ll 1$, we have

$$\begin{aligned} K_{hh}(\eta) &\approx -\frac{18}{5\pi^{3/2}}(\ln|\eta| + \gamma_h), \\ K_{hp}(\eta) &\approx \frac{1}{5}, \\ K_{pp}(\eta) &\approx -\frac{4}{5\pi^{1/2}}(\ln|\eta| + \gamma_p), \end{aligned} \tag{17}$$

where γ_h and γ_p are constants. For K_{hR}, K_{RR}, and $K_{R\pi}$ (friction related kernels), the asymptotic forms do not exist. However, the corresponding closures vanish in the collisionless limit and extrapolations of the 6400-moment kernels are accurate enough.

Putting all of this together, the kernel functions can be fitted to a single function

$$K_{AB}(\eta) = -[d + a\exp(-b\eta^c)]\ln[1 - \alpha\exp(-\beta\eta^\gamma)] \tag{18}$$

with parameters *a, b, c, d,* α, β, and γ listed in Table I. The fitted kernels are plotted in Fig. 1 and the corresponding closure moments due to sinusoidal drives in Fig. 2. Note that the fitted kernels reproduce closure values in the collisional ($k \to 0$) and collisionless ($k \to \infty$) limits.

IV. DISCUSSION

We have presented a complete set of electron parallel closures with ion charge $Z = 1$ for arbitrary collisionality, Eqs. (2)-(4) and Table I. Generalization to arbitrary Z is straightforward. Ion parallel closures can also be obtained similarly for varying electron-ion temperature ratios.

	a	b	c	d	α	β	γ
K_{hh}	-5.32	0.170	0.646	6.87	1	2.02	0.417
K_{hR}	6.37	5.12	0.160	0.100	1	1	0.583
$K_{h\pi}$	-0.229	2.26	0.594	0.363	0.775	1.49	0.478
K_{RR}	245	8.06	0.147	0.432	1	3.40	0.347
$K_{R\pi}$	-0.226	3.21	0.678	0.696	1	3.40	0.347
$K_{\pi\pi}$	0.724	0.932	0.654	0.195	1	1.60	0.491

Table I: Fitted parameters for kernel function $K_{AB}(\eta) = -[d + a\exp(-b\eta^c)]\ln[1 - \alpha\exp(-\beta\eta^\gamma)]$.

Efforts to obtain analytic expressions for these cases are ongoing and will be presented in the near future.

Closing fluid equations using the integral closures presented here is computationally feasible in simulations of astrophysical and laboratory plasmas. Although the implementation of such closures benefits from field-line aligned coordinates (BOUT++ [17]), plasma fluid codes that do not have field-line aligned grids (e.g., NIMROD [18]) may still benefit from the added efficiency of evaluating simple fitted kernels. The practicability of three dimensional fluid simulations with integral closures is shown in Ref. [10] and discussed in Ref. [12].

Acknowledgments

One of authors (Ji) would like to thank Dr. Hogun Jhang for general discussions of using the integral closures and Dr. Dongcheol Seo for discussing the fitting method. The research was supported by the U.S. DOE under grant Nos. DE-FG02-04ER54746, DE-FC02-04ER54798 and DE-FC02-05ER54812 and by the World Class Institute (WCI) Program of the National Research Foundation of Korea (NRF) funded by the Ministry of Education, Science and Technology of Korea (MEST) (NRF Grant No. WCI 2009-001). This work is performed in conjunction with the Plasma Science and Innovation (PSI) center and the Center for Extended Magnetohydrodynamics. This research used resources of the National Energy Research Scientific Computing Center, which is supported by the Office of Science of the U.S. Department of Energy under Contract No. DE-

AC02-05CH11231.

[1] S. I. Braginskii, in *Reviews of Plasma Physics*, edited by M. A. Leontovich (Consultants Bureau, New York, 1965), vol. 1, p. 205.

[2] G. W. Hammett and F. W. Perkins, Phys. Rev. Lett. **64**, 3019 (1990).

[3] R. D. Hazeltine, Phys. Plasmas **5**, 3282 (1998).

[4] P. B. Snyder, G. W. Hammett, and W. Dorland, Phys. Plasmas **4**, 3974 (1997).

[5] Z. Chang and J. D. Callen, Phys. Fluids B **4**, 1167 (1992).

[6] E. D. Held, J. D. Callen, C. C. Hegna, and C. R. Sovinec, Phys. Plasmas **8**, 1171 (2001).

[7] E. D. Held, Phys. Plasmas **10**, 4708 (2003).

[8] J.-Y. Ji and E. D. Held, Phys. Plasmas **13**, 102103 (2006).

[9] J.-Y. Ji and E. D. Held, Phys. Plasmas **15**, 102101 (2008).

[10] J.-Y. Ji, E. D. Held, and C. R. Sovinec, Phys. Plasmas **16**, 022312 (2009).

[11] J.-Y. Ji and E. D. Held, J. Fusion Energy **28**, 170 (2009).

[12] J. T. Omotani and B. D. Dudson, Plasma Phys. Control. Fusion **55**, 055009 (2013).

[13] J.-Y. Ji, E. D. Held, and H. Jhang, Phys. Plasmas **20**, 082121 (2013).

[14] R. D. Hazeltine, Plasma Phys. **15**, 77 (1973).

[15] J.-Y. Ji and E. D. Held, Phys. Plasmas **21**, 042102 (2014).

[16] J.-Y. Ji and E. D. Held, Phys. Plasmas **20**, 042114 (2013).

[17] B. D. Dudson, M. V. Umansky, X. Q. Xu, P. B. Snyder, and H. R. Wilson, Comput. Phys. Comm. **180**, 1467 (2009).

[18] C. R. Sovinec, A. H. Glasser, T. A. Gianakon, D. C. Barnes, N. R. A., S. E. Kruger, D. D. Schnack, S. J. Plimpton, A. Tarditi, M. S. Chu, et al., J. Comp. Phys. **195**, 355 (2004).